

Propagation Modelling and Measurements in a Populated Indoor Environment at 5.2 GHz

K. I. Ziri-Castro⁺, N. E. Evans[#] and W. G. Scanlon^{*}

⁺*Department of Mathematics and Computing, University of Southern Queensland, West Street, Toowoomba, Queensland, 4350, Australia.*

[#]*School of Electrical and Mechanical Engineering, University of Ulster, Shore Road, Newtownabbey, Northern Ireland, BT37 0QB, UK.*

^{*}*School of Electrical and Electronic Engineering, The Queen's University of Belfast, Ashby Building, Stranmillis Road, Belfast, Northern Ireland, BT9 5AH, UK.*

ziricast@usq.edu.au

Abstract

Human occupants within indoor environments are not always stationary and their movement will lead to temporal channel variations that strongly affect the quality of indoor wireless communication systems. This paper describes a statistical channel characterization, based on experimental measurements, of human body effects on line-of-sight indoor narrowband propagation at 5.2 GHz. The analysis shows that, as the number of pedestrians within the measurement location increases, the Ricean K-factor that best fits the empirical data tends to decrease proportionally, ranging from $K=7$ with 1 pedestrian to $K=0$ with 4 pedestrians. Level crossing rate results were Rice distributed, while average fade duration results were significantly higher than theoretically computed Rice and Rayleigh, due to the fades caused by pedestrians. A novel CDF that accurately characterizes the 5.2 GHz channel in the considered indoor environment is proposed. For the first time, the received envelope CDF is explicitly described in terms of a quantitative measurement of pedestrian traffic within the indoor environment.

1. Introduction

There is a number of significant radio wave propagation phenomena present in the populated indoor environment, including multi-path fading and human body effects. The latter includes shadowing and scattering caused by pedestrian movement, and antenna-body interaction with body-worn or hand portable terminals [1]. Human occupants within indoor environments are not always stationary and their movement will lead to temporal channel variations. Hence, populated environments remain a major challenge for wireless local area networks (WLAN) and other indoor communication systems. Therefore, it is important to develop an understanding of the potential and

limitations of indoor radio wave propagation at key frequencies of interest, such as the 5.2 GHz band employed by commercial WLAN standards such as IEEE 802.11a.

Although several indoor channel propagation studies have been reported in the literature, see Section II, these temporal variations have not yet been thoroughly investigated. Therefore, we have made an important contribution to the area by conducting a systematic study of the problem, including a propagation measurement campaign and statistical channel characterization.

Measurements were performed in the everyday environment of a 7.2 m wide University hallway to determine the statistical characteristics of the 5.2 GHz channel for a fixed, transverse line-of-sight (LOS) link perturbed by pedestrian movement. Data were acquired at hours of relatively high pedestrian activity, between 12.00 and 14.00. The location was chosen as a typical indoor wireless system environment that had sufficient channel variability to permit a valid statistical analysis.

The paper compares the first and second order statistics of the empirical signals with the Gaussian-derived distributions commonly used in wireless communications. From these results, a novel statistical model was derived that describes the characteristics of the received envelope as a function of indoor pedestrian activity. An explicit equation for the novel cumulative distribution function (CDF) was derived by performing regression modeling of the empirical data.

The remainder of this paper is organized as follows. Section 2 presents a comprehensive survey of previous studies of human body effects on radio wave propagation. Section 3 provides a detailed description of the experimental setup used for the LOS measurements; the latter are compared with standard first and second order statistical distributions in Section 4. Section 5 presents the new statistical model, while Section 6 summarizes the work and makes suggestions for future research.

2. Radio Propagation in Populated Indoor Environments

As the elevation of base stations and associated terminals is usually much lower in indoor environments than in outdoor communication systems, the propagation loss by body shadowing greatly affects the received signal strength and can significantly degrade transmission quality [2], [3]. Moving pedestrians can intersect the direct path between the transmitting and receiving antennas, potentially blocking the LOS path. Often, as the propagation conditions become non-LOS (NLOS), the communication link can be maintained by the contribution of reflected waves in the environment. In addition, local moving pedestrians may act as additional scatterers, contributing to multipath fading through a combination of reflection and diffraction mechanisms.

Doppler effects are not significant when considering pedestrian movement, due to the relatively low speeds involved. The maximum change in frequency that the received signal will experience due to reflections from human bodies that are in relative motion between the transmitter and receiver, i.e., the maximum Doppler shift, is the ratio between the relative speed of the human body and the signal wavelength. In this work we have considered the speed of the human body as the speed of the pedestrian torso, neglecting additional velocity components caused by movements of arms and legs. For example, even with a pedestrian almost running, at 2 m/s, the resultant maximum Doppler shift at 5.2 GHz is only 34.5 Hz, causing slow-fading effects. A more typical walking speed is around 0.5 m/s.

It is important to consider that indoor propagation is also very strongly influenced by a number of environmental factors: the relative locations of transmit and receive antennas, the layout of the particular building under consideration, and the constructional materials used for the walls, floors and ceilings. Both measured and simulated data studied by Otmani et al. [4] reveal an important site-dependent, multi-ray propagation process. The basic room structure and furniture serve as scatterers of the propagating wave. However, when terminals are stationary, the main cause of temporal fading in populated indoor environments is the movement of people [5], [6]. Results for fixed terminals operating from 914 MHz up to 4 GHz within buildings are reported in [7]. The measurements revealed that ambient motion by people throughout the building caused Ricean fading, with a Rice K factor of approximately 10.

Temporal variations due to human body-shadowing and multipath in indoor radio channels were also studied by Bultitude *et al.* who described measurements for fixed

receiver locations. The measurements, at 890 MHz [8] and at 910 MHz [9], were made during office hours when there was movement of personnel along the rooms (hallways and office) where the receiver was situated. They found that, in these environments, signal fade occurred in bursts of one or two seconds duration, interspersed by periods during which the received signal remained almost constant. The CDF of the received signal envelope was Ricean for N-LOS transmission.

Tang et al. [10] studied the effects of people and other moving objects by performing measurements at 1.9 GHz in hallways and large closed-in areas. Fades with more than 10 dB magnitude were observed. The distribution of the fading signal was found to be lognormal. As a consequence, deeper fading was more likely to be observed when there was more pedestrian activity.

In [11], the results of carrier wave temporal fading measurements at 1100 MHz in a modern office environment under diversified sets of conditions were reported. The effects of controlled degrees of motion with up to 4 individuals walking around the transmitter and the receiver antennas were investigated. Hashemi concluded that the Nakagami distribution provided the best fit to envelope fading for most cases. More recently, Stoytchev *et al.* [12] studied the temporal behavior of a single transmit wireless channel inside buildings at 2.8 GHz. They performed measurements of the received power and electric field strength in metal-wall and brick-wall environments. They found that the statistics of long-term variations of the received power were well described by a Ricean model with a K factor of approximately 10.

Notwithstanding the measurement campaigns performed to date, there seems to be no conclusive results to describe the behavior of the populated indoor propagation channel. The probability distribution of the received signal envelope was found to be Ricean in the majority of the experiments reported. However, Weibull, Nakagami and lognormal distributions were also found to describe the received envelope in some cases. Furthermore, the relationship between pedestrian traffic density and statistical characteristics of the received envelope has not yet been thoroughly investigated.

3. Experimental Set-Up

A block diagram of the narrowband measurement system is shown in Figure 1. The transmitter (TX) consisted of a vector signal generator, a GaAs passive frequency doubler, a high efficiency GaAs InGaP power amplifier, and a sleeve dipole antenna (+2.2 dBi). The TX was

adjusted to deliver +10 dBm to the antenna input port, taking account of cable losses. The transmitter system was placed on a wheeled cart to facilitate movement around the measurement location.

The 5.2 GHz receiver module (RX) had a custom RF unit, a 12-bit analogue to digital converter (ADC) and a notebook PC for data recording. The receive antenna was a sleeve dipole identical to the one used at the transmitter. The custom RF unit was single conversion with two tuned RF gain stages, a 915 MHz IF strip, and a logarithmic detector delivering an output voltage, V_{out} (in mV), almost linear with received input power in dBm. The measured RF performance parameters of the custom RF unit are given in Table 1. A more detailed description of the measurement system has been reported in [19]. V_{out} was sampled at 5 ms intervals using the ADC and the results stored on the notebook PC. The measured power results include the effect of both transmit and receive antenna gains.

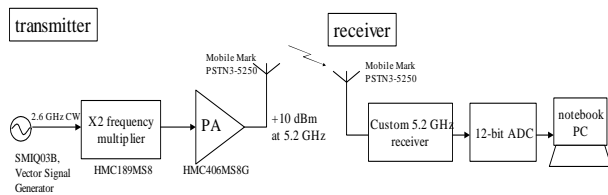


Figure 1: Block diagram of narrowband 5.2 GHz measurement system.

The measurement location was a broad central hallway, located on the second floor of a university building. The area considered was a section measuring 13.7 m by 7.18 m, see Figure 2, with large windows along the entire length of the two sidewalls. The overall hallway length extended in both directions to well over 70 m, so effectively there were no end walls. The sidewalls were constructed from painted concrete blocks and the floor was covered with commercial grade polypropylene carpet. The ceiling was suspended at a height of 2.75 m. It was composed of mineral tiles and recessed louvered luminaries. The ceiling void was 0.5 m high.

The transmit antenna was vertically polarized and mounted 1.4 m above floor level, and 0.9 m from the sidewall, on a wheeled cart. The RX was positioned 0.85 m above floor level, and 0.3 m from the sidewall, on a wooden support. The offset dimensions were measured relative to the TX and RX antenna feed positions.

A digital video camera was fixed at one side of the TX to record pedestrian activity across the link. The camera was set 1.4 m above floor level and 0.9 m from the TX. Pedestrian traffic across the LOS was recorded at 30

frames per second, in sessions of 5 minutes duration. Hence, the time resolution for the digital video data is 33 ms per frame; at an estimated average pedestrian speed of 0.5 m/s this is equivalent to a pedestrian movement of 1.65 cm (0.29λ at 5.2 GHz).

Table 1: Specification and measured performance for receiver custom RF unit.

Parameter	Value	Comment
Intermediate Frequency (IF)	915 MHz	Single conversion
IF bandwidth	25 MHz	Nominal
Front end gain	20.2 dB	Includes IL for bandpass filters and mixer
Effective noise floor	-96 dBm	
Range of input power for linear output	-23 dBm to -88 dBm	65 dB dynamic range (± 1 dB error)
Output sensitivity	46 mV/dB	V_{out} : 1.2 V to 4.6 V

To quantitatively measure the degree of pedestrian traffic, a discrete variable was manually extracted from the digital video data to represent the number of pedestrians present in the measurement location at a certain time; this is denoted as $n(t)$. Figure 3 shows an example of a video frame taken in the measurement location in which $n(t) = 4$. From now on, we will refer to $n(t)$ as simply n .

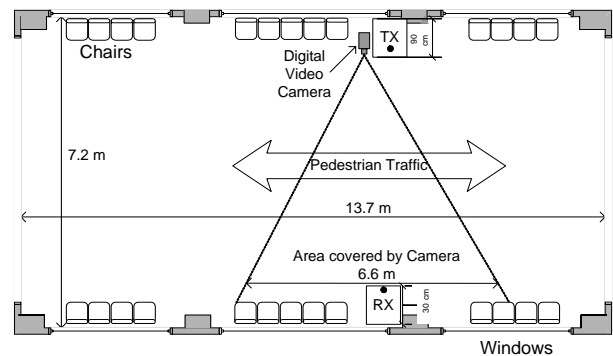


Figure 2 Measurement location (university hallway) layout.

During the measurements, all pedestrians walked freely and there was no control over trajectory or speed.

However, the natural geometry of the location allowed pedestrian traffic to flow along the hallway in directions predominantly perpendicular to the link, as shown in Figure 2 and 3.



Figure 3 Example of a video frame with 4 pedestrians within the measurement area ($n(t1) = 4$).

4. Experimental Results

4.1. Received Power

A total of 15 minutes (3 sessions of 5 minutes each) were used for the analysis presented here, comprising a total of 180 Ksamples of received power at a 5 ms sampling interval. To determine the effective noise floor for this location, time, frequency band and measurement system, received power measurements were made with the TX switched off just prior to the experiment. For 5 minutes (60 Ksamples), the averaged measured noise floor was -82.0 dBm, with a standard deviation of 0.7 dB. The lowest received power value during the 15 minutes time series analysis was -73.2 dBm. This value is well above both the measured sensitivity level of the RX unit (-88.0 dBm), and the measured noise floor for this location.

A 40-s example of the received power profile and associated pedestrian traffic characterization against time is given in Figure 4. Summary statistics for the received power show that there were no significant variations in the averaged, maximum, and minimum values of the received power as the number of pedestrians present within the measurement area (n) increases. A fuller analysis, including first and second order statistics, is needed to determine whether or not the variations in n will affect the statistical characteristics of the received envelope.

4.2. First Order Statistics

The second and following pages should begin 1.0 inch (2.54 cm) from the top edge. On all pages, the bottom margin should be 1-1/8 inches (2.86 cm) from the bottom edge of the page for 8.5 x 11-inch paper; for A4 paper, approximately 1-5/8 inches (4.13 cm) from the bottom edge of the page.

A description of the channel in terms of probability distribution functions is usually adequate for the evaluation of narrowband systems [15]-[18]. Therefore, we compared the empirical CDFs with the Rayleigh, Rice and Lognormal distributions.

The Rice factor (K) is defined as the ratio of powers of the dominant (specular, or coherent) component, r_s , and the Rayleigh component of the received envelope (r). K tends to zero as the dominant component r_s approaches zero dB and the distribution becomes Rayleigh, while as r_s tends to infinity, the envelope approaches the Gaussian distribution, with mean r_s . Therefore, the Rice K factor is a parameter that indicates the transition between the Rayleigh and the Gaussian cases.

The Rice CDF can be expressed as:

$$P(r \leq R) = 1 - Q_1\left(\frac{r_s}{\sigma}, \frac{R}{\sigma}\right) \quad (1),$$

where the Marcum Q function [22] is defined as

$$Q_1(a, b) = \int_b^{\infty} x e^{-(x^2+a^2)/2} I_0(ax) dx \quad (2).$$

where $I_0(\cdot)$ designates the zeroth-order modified Bessel function of the first kind.

To study in more detail how the signal characteristics changed with the number of pedestrians in the measurement area (n), the statistics of the overall received signal for the entire 15 minutes series were separately analyzed with respect to n .

Figure 5 shows the CDF of the received signal as n increases, theoretical Rayleigh and Rice ($K = 3, 7, 15, 20$ and 40) distributions are For the case with no pedestrians, the received envelope tended to be Rice distributed with a K factor ranging between 15 and 20. However, for $n > 0$ the empirical CDFs were both distinct from each other and significantly different to Rice, Rayleigh or Lognormal distributions. As n increased, the CDF slope near the median tended to decrease proportionally, equivalent to a decreasing K factor in a Rice distribution. This is attributed to additional direct ray attenuation in the received envelope as n increased. For a higher number of pedestrians ($n = 5$) the CDF was more similar to the lognormal distribution, particularly for values below the median. The Nakagami distribution models the Rice, Rayleigh, and lognormal distributions in terms of

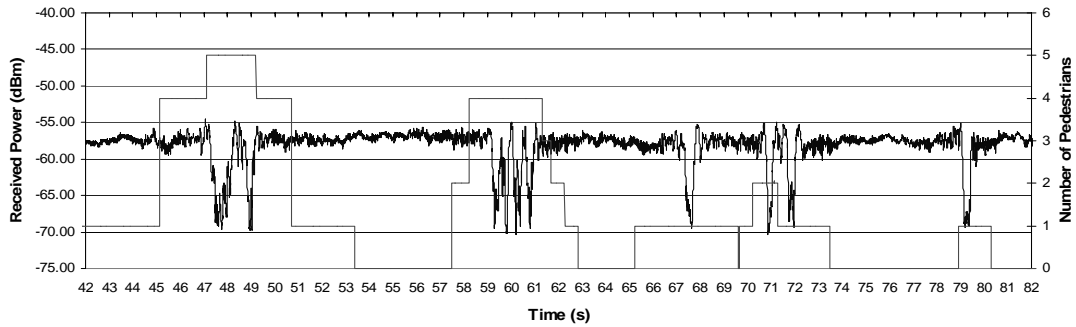


Figure 4 Example of received profile and associated pedestrian traffic, showing the number of pedestrians within the measurement area ($n(t)$).

the parameter m [18]. The lognormal distribution is obtained with $m = 0.5$, Rayleigh with $m = 1$, and Rice distributions correspond to higher values of m . Then, it seems to be an inversely proportional relationship between the m factor of the Nakagami distribution and the slope near the median of the empirical CDFs as n increases. These results are entirely consistent with measurement results obtained for controlled scenarios described for a fixed link at 5.2 GHz in previous work [19], where the K factor reduced as the number of pedestrians within the measurement area increased.

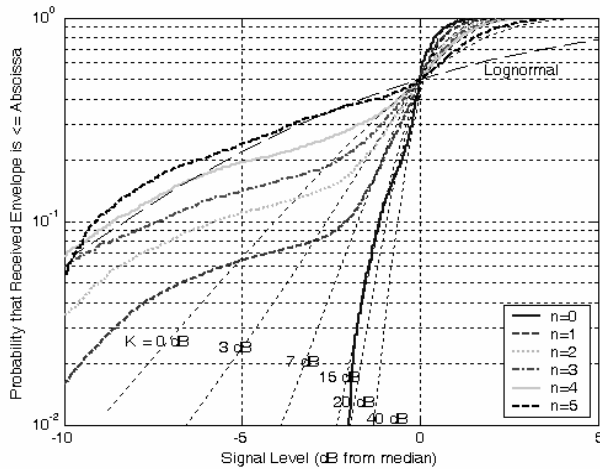


Figure 5: CDF of the received envelope (15 minute series) as n increases. Rayleigh and Rice distributions are shown for reference.

4.3. Second Order Statistics

Second order statistics are expressed as the level-crossing rate (LCR), defined as the rate at which the envelope crosses a specified level in a positive-going direction, and the average fade duration (AFD), the average time for which the received envelope is below that specified level.

Figure 6 shows that, as the number of pedestrians within the measurement area increased, the maximum LCR also increased. This indicates that, as the number of moving pedestrians within the measurement area increases, the variations in the received envelope also tend to increase. The AFD results below the mean for $1 \leq n \leq 5$ were higher than theoretically computed Rice and Rayleigh AFD, due to the fades caused by pedestrians when blocking the LOS.

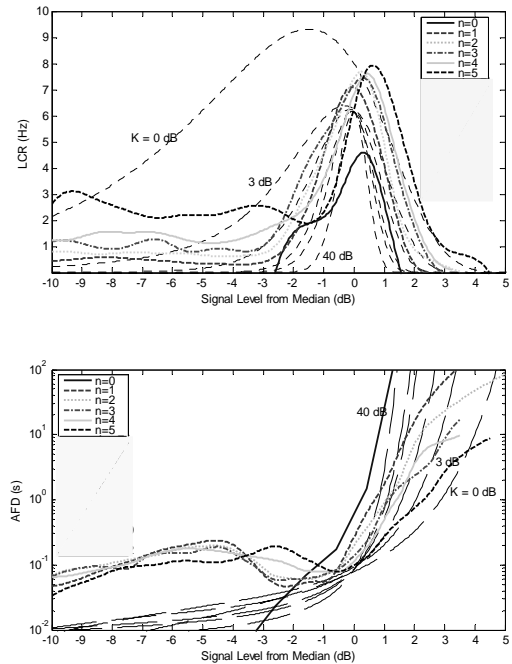


Figure 6: LCR and AFD results with respect to local mean for the received envelope (15 minute series), as n increases. Rayleigh and Rice distributions are shown for reference.

5. A Novel Statistical Model for Populated Indoor Environments

To generate a mathematical model for the CDFs depicted in Figure 5, let us define $\Xi = \{\xi_n\}, n \in \{1, \dots, N\}$ as a set of possible mappings, associated with a finite number of observed empirical CDFs $\{\xi_n\}$, where n is the number of pedestrians in the measurement location.

Particularly, for the results given in Figure 5, let us restrict the maximum observed number of pedestrians n to $N=5$. In this figure, a consistent behavior in terms of the number of pedestrians, n , was observed. Therefore, it is feasible *i*) to explore possible mathematical models for the empirical CDFs, and *ii*) to investigate possible mappings between the symbolical CDF models and the empirical CDFs.

As a modeling strategy for every empirical CDF ξ_n , it is possible to regress a linear combination of a finite set of mappings $\Psi_n = \{\psi_i(r)\}, \forall i > 0 \in \mathfrak{N}, \forall n \in \{1, \dots, 5\}$, r being the CDF argument (normalized received envelope in dBm). By visual inspection of the empirical CDFs in Figure 5, it is logical to restrict Ψ_n to

$$\Psi_n = \{\alpha, r, \mathcal{Q}_1(r_r)\} \quad (3)$$

where r_r is the received faded envelope, $\alpha \in \mathfrak{R}$ is an independent term, and $\mathcal{Q}_1(\cdot)$ is an approximation to the Marcum Q function, $\mathcal{Q}_1(\cdot)$, proportional to the error function, $erfc(\cdot)$ [21]. In this framework, α and r will accommodate monotonically linear variations of the ‘core’ non-linear mapping $\mathcal{Q}_1(r_r)$. Such a non-linear mapping is suggested since there has been evidence, throughout findings reported in [21], that the empirical CDFs $\{\xi_n\}$ contain non-linear core mappings of the Rice distribution. Note that the Marcum Q function is the integral of the Rice envelope, see Equation (4).

The Marcum Q function can also be expressed in terms of two variables, a_1 , and a_2 , representing power quantities as in [21]:

$$Q(a_1, a_2) \sim erfc\left(\frac{a_2 - a_1}{\sqrt{2}}\right), \quad a_2 \gg 1, a_2 \gg a_2 - a_1 \quad (4)$$

For the empirical CDFs, the amplitude of the received envelope, r_r , can be approximated to $|R| - |r_s|$. Since R is

the absolute Rice envelope, $R^2 = r_s^2 + r_r^2$, where r_s is the envelope of the specular component.

It is then possible to restrict the multivariable mapping in (7) to one-dimensional form, giving:

$$Q_1\left(\frac{r_s}{\sigma}, \frac{R}{\sigma}\right) \sim erfc\left(\frac{r_r}{\sqrt{2}}\right) = \mathcal{Q}_1(r_r), \quad |R| \gg 1, |R| \gg |r_s| \quad (5)$$

Therefore, it makes sense to use $\mathcal{Q}_1(r_r)$ as a core non-linear mapping in Ψ_n .

To find all $N = 5$ mappings in Ξ , the regression problem can be solved for the set of mappings of the form

$$\xi_n = \alpha_n + \beta_n r + \delta_n \mathcal{Q}_1(r_r), \quad \alpha_n, \beta_n, \delta_n \in \mathfrak{R}, \quad n \in \{1, \dots, 5\} \quad (6)$$

For convenience, let us introduce a vector notation for (9), as follows:

$$\begin{bmatrix} \xi_1 \\ \xi_2 \\ \vdots \\ \xi_N \end{bmatrix} = \begin{bmatrix} \alpha_1 & \beta_1 & \delta_1 \\ \alpha_2 & \beta_2 & \delta_2 \\ \vdots & \vdots & \vdots \\ \alpha_N & \beta_N & \delta_N \end{bmatrix} \begin{bmatrix} 1 \\ r \\ \mathcal{Q}_1(r_r) \end{bmatrix} = \mathbf{A} \begin{bmatrix} 1 \\ r \\ \mathcal{Q}_1(r_r) \end{bmatrix} \quad (7)$$

Given the empirical CDF data, multiple regression solves for the unknown coefficients α_n , β_n , and δ_n by performing a least-square fit. Hence, the solution for the regression matrix A is as follows:

$$\mathbf{A} = \begin{bmatrix} 0.9921 & 0.0064 & -0.7544 \\ 0.9410 & 0.0130 & -0.4525 \\ 0.9126 & 0.0152 & -0.3867 \\ 0.8798 & 0.0237 & -0.3503 \\ 0.7889 & 0.0342 & -0.1927 \end{bmatrix} \quad (8)$$

The model presented in (10) and (11) is graphically presented in Figure 7 where it is observed that the mappings in (11) are a good fit for the empirical data. This can be corroborated by applying a Wilcoxon rank sum test, which verifies that two population means are identical only if p value > 0.1 . The p -values, were computed for all cases, $n = 1, \dots, 5$, giving:

$$[p_1, \dots, p_5] = [0.857, 0.224, 0.298, 0.233, 0.443] \quad (9)$$

It is desirable now to generalize the model presented in (10), in terms of the number of pedestrians n . Firstly, define $z \in [1, 5]$ as the ‘continuous’ number of pedestrians.

Let us now define a novel cumulative distribution function, $cdfPT(r, z)$, which predicts the probability of a received signal in terms of the received envelope, r , and the number of pedestrians, z , as follows:

$$cdfPT(r, z) = Prob(r \leq r_0, z = [1,5]) \quad (10)$$

which will serve as a continuous generalization, $z \in [1,5]$, of the set Ξ by incorporating pedestrian traffic.

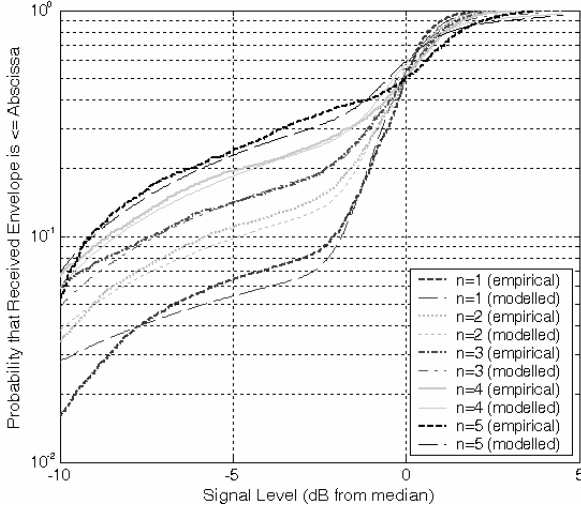


Figure 7. Proposed and empirical CDFs.

The $cdfPT$ can be found by computing the linear least square fits, $h_\alpha(z)$, $h_\beta(z)$, and $h_\delta(z)$, for every column in the regression matrix A (11) by incorporating them in (9), as follows:

$$cdfPT(r, z) = h_\alpha(z) + h_\beta(z)r + h_\delta(z)\mathcal{Q}_1(r), \quad z \in [1,5] \quad (11)$$

After computing the linear regression for $h_\alpha(z)$, $h_\beta(z)$, and $h_\delta(z)$, the general form for $cdfPT(r, z)$ can be found

$$cdfPT(r, z) = \nu_0 + \nu_1 z + (\nu_2 + \nu_3 z)r + (\nu_4 + \nu_5 z)\mathcal{Q}_1(r), \quad \nu_i \in \mathfrak{R}, \quad i \in \{1, \dots, 5\} \quad (12)$$

where, for the data considered in this chapter, the coefficients ν_i take the following values:

$$\begin{bmatrix} \nu_0 \\ \nu_1 \\ \nu_2 \\ \nu_3 \\ \nu_4 \\ \nu_5 \end{bmatrix} = \begin{bmatrix} 1.0432 \\ -0.0467 \\ -0.0013 \\ 0.0066 \\ -0.5194 \\ 0.0617 \end{bmatrix} \quad (13)$$

It is interesting to note that the coefficients that multiply the function $\mathcal{Q}_1(r)$ in (9), and (15), verify the following:

$$\delta_n = (\nu_4 + \nu_5 z) < 0, \quad \forall n \in [1,5]$$

which is consistent with the CDF for a Rice envelope, see equation (4).

The multivariate CDF, $cdfPT(r, z)$, model the behavior of the empirical CDF in the light of a theoretical continuous distribution of pedestrian traffic.

6. Conclusions

A novel empirical statistical model was proposed to predict the effect of pedestrian movement for a LOS narrowband 5.2 GHz link within a university mall. Based on the Rice distribution, this new CDF describes the cumulative probability for the received envelope of the empirical data in terms of a quantitative measurement of pedestrian traffic within the indoor environment. A CDF that exclusively depends on the received power and number of pedestrians within the measurement environment was formulated.

The results presented firmly verify the significance that human body propagation effects have on the indoor communications channel at 5.2 GHz. Although there were no distinctive variations in the instant averaged, maximum, and minimum values of the received power, significant variations were detected in both first and second order statistics as the number of pedestrians within the measurement area increased. The slope of the empirical CDFs near the median tended to decrease proportionally with the number of pedestrians. LCR results were Rice distributed, considering a maximum Doppler frequency of 8.67 Hz. AFD results below the mean were significantly higher than theoretically computed Rice and Rayleigh, due to the fades caused by pedestrians when blocking the LOS.

The proposed empirical model provides an insight into the prediction of human body shadowing effects for indoor channels at 5.2 GHz. The next phase of this work will address measurements under different scenarios including mobile and bodyworn terminal effects.

References

- [1] W. G. Scanlon and N. E. Evans, "Numerical analysis of bodyworn UHF antenna systems," *IEE Electronics & Communication Engineering Jnl.*, vol. 13, pp. 53–64, April 2001.
- [2] K. Sato and T. Manabe, "Estimation of propagation-path visibility for indoor wireless LAN systems under shadowing condition by human bodies," in *Proc. IEEE 48th Veh. Technol. Conf.*, vol. 3, Ottawa, Canada, May 1998, pp. 2109–2113.
- [3] S. Obayashi and J. Zander, "A body-shadowing model for indoor radio communication environments," *IEEE Trans. Antennas Propagat.*, vol. 46, pp. 920–927, Jun. 1998.

- [4] M. Otmani and M. Lecours, "Indoor Radio Measurements and Simulations with Polarization Diversity," *Wireless Pers. Commun.*, vol. 3, no. 3, pp. 243–256, 1996.
- [5] Y. Yamaguchi, A. Takeo and T. Sekiguchi, "Radio Propagation Characteristics in Underground Streets Crowded with Pedestrians," *IEEE Trans. Electromagn. Compat.*, vol. 30, pp. 130–136, May 1988.
- [6] P. Marinier, Y. Delisle and C.L. Despins, "Temporal Variations of the Indoor Wireless Millimeter-Wave Channel," *IEEE Trans. Antennas Propagat.*, vol. 46, pp. 928–934, Jun. 1998.
- [7] J. Andersen, T. Rappaport and S. Yoshida, "Propagation Measurements and Models for Wireless Communication Channels," *IEEE Communicat. Mag.*, vol. 1, pp. 42–49, Jan. 1995.
- [8] R. Bultitude, G. Bedal and J. Powell, "Propagation Characteristics of 800/900 MHz Radio Channels Operating Within Buildings," in *Proc. 13th Biennial Symp. on Communications*, Jun., 1986, pp. B.1.1–B.1.4.
- [9] R. J. C. Bultitude, "Measurement, characterization and modeling of indoor 800/900 MHz radio channels for digital communications," *IEEE Communicat. Mag.*, vol. 25, pp. 5–12, Jun. 1987.
- [10] Y. Tang and H. Sobol, "Measurements of PCS Microwave Propagation in Buildings" *Applied Microwave and Wireless*, vol. 7, pp. 38.40.43–60, Winter 1995.
- [11] H. Hashemi, "A Study of Temporal and Spatial Variations of the Indoor Radio Propagation Channel," in *Proc. IEEE 5th Int. Symp. on Personal Indoor and Mobile Radio Comm.*, vol. 1, Sept. 1994, pp. 127–134.
- [12] M. Stoytchev, H. Safar, "Statistics of the Temporal Variations in the Wireless Transmission Channel in Indoor Environments," in *Proc. MPRG Symp. Wireless Personal Comm.*, Jun. 2000, pp. 1–10.
- [13] J.D. Parsons, "The Mobile Radio Propagation Channel," John Wiley & Sons, Ltd., 2000.
- [14] M. Tobin, J. Richie, "Indoor Propagation: A Statistical Approach," in *Proc. Electromagnetic Environments Conseq. Euroem.*, vol. 2, pp. 1301–1308, 1994.
- [15] H. Hashemi, "The Indoor Propagation Channel," in *Proc. of the IEEE*, vol. 81, Jul. 1993, pp. 941–968.
- [16] A. F. Abbouraddy and S. M. Elnoubi, "Statistical Modeling of the Indoor Radio Channel at 10 GHz Through Propagation Measurements—Part I: Narrow-Band Measurements and Modeling," *IEEE Trans. Veh. Technol.*, vol. 49, pp. 1491–1507, Sept. 2000.
- [17] J. I. Marcum, "A statistical theory of target detection by pulsed radar," *IRE Transactions*, IT-6, pp. 59–267, April 1960.
- [18] M. Nakagami, "The m-distribution – a general formula of intensity distribution of rapid fading," in W.C. Hoffman (ed.), *Statistical methods in radio wave propagation*, Pergamon, Oxford, 1960.
- [19] K. Ziri-Castro, W. G. Scanlon, and N. E. Evans, "Characterisation of body shadowing effects in the indoor environment at 5.2 GHz," in *Proc. IEEE 8th High Frequency Postgraduate Student Colloquium*, Sept. 2003, pp. 2–5.
- [20] W.C. Jakes, *Microwave Mobile Communications*. Ed. by W. C. Jakes, Jr. New York; London: Wiley-Interscience, 1974.
- [21] G. L. Stüber, "Principles of Mobile Communication," 2nd ed., Kluwer Academic Publishers, 2001.
- [22] Vaughan, and J. B. Andersen, "Channels, Propagation and Antennas for Mobile Communications," *The Institution of Electrical Engineers*, London, UK. 2003.
- [23] R. Feustle, "Miniature 5.2 GHz Power Measurement Receiver," MEng Thesis. University of Ulster. May 2002.